In search of superluminal quantum communications: recent experiments and possible improvements

2013 J. Phys.: Conf. Ser. 442 012005

(http://iopscience.iop.org/1742-6596/442/1/012005)

In search of superluminal quantum communications: recent experiments and possible improvements.

B Cocciaro[1], S Faetti[2] and L Fronzoni[2]

[1] High School XXV Aprile, Via Milano 2, I-56025 Pontedera (Pisa), Italy
[2] Department of Physics Enrico Fermi, Largo Pontecorvo 3, I-56127 Pisa, Italy

E-mail: b.cocciaro@comeg.it, faetti@df.unipi.it, fronzoni@df.unipi.it

Abstract. As shown in the famous *EPR* paper (Einstein, Podolsky e Rosen, 1935), Quantum Mechanics is non-local. The Bell theorem and the experiments by Aspect and many others, ruled out the possibility of explaining quantum correlations between entangled particles using local hidden variables models (except for implausible combinations of loopholes). Some authors (Bell, Eberhard, Bohm and Hiley) suggested that quantum correlations could be due to superluminal communications (tachyons) that propagate isotropically with velocity $v_t > c$ in a preferred reference frame. For finite values of v_t, Quantum Mechanics and superluminal models lead to different predictions. Some years ago a Geneva group and our group did experiments on entangled photons to evidence possible discrepancies between experimental results and quantum predictions. Since no discrepancy was found, these experiments established only lower bounds for the possible tachyon velocities v_t. Here we propose an improved experiment that should lead us to explore a much larger range of possible tachyon velocities v_t for any possible direction of velocity $\vec{V}$ of the tachyons preferred frame.

1. Introduction

The non local character of Quantum Mechanics (QM) has been object of a great debate starting from the famous Einstein-Podolsky-Rosen (EPR) paper [1]. Consider, for instance, a quantum system made by two photons a and b that are in the polarization entangled state

$$|\psi >= \frac{1}{\sqrt{2}} \left(|H, H > + e^{i\phi} |V, V > \right) \tag{1}$$

where H and V stand for horizontal and vertical polarization, respectively, and ϕ is a constant phase coefficient. The two entangled photons are created at point O, propagate in space far away one from the other (see Fig.1) and reach at the same time points A and B that are equidistant from O as schematically drawn in Fig.1.

Suppose the polarization of the two photons is measured at the same time at points A and B. According to QM, a measurement of horizontal polarization of photon a (or b) leads to the collapse of the entangled state to $|H, H >$, then, also photon b (or a) must collapse to the horizontal polarization. This behaviour suggests the existence of a sort of "action at a distance" qualitatively similar to that introduced in the past to describe interactions between either electric charges or masses. However, according to the Maxwell electromagnetic theory and to the Einstein General Relativity theory, it is now commonly accepted that interactions between electric charges or masses are not instantaneous but occur through exchange of signals

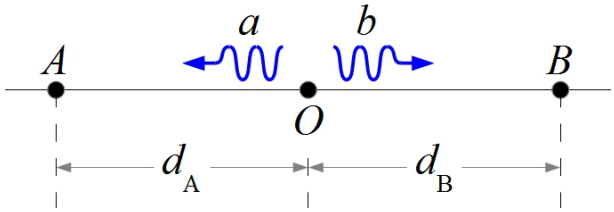

Figure 1: O: point where a couple of entangled photons (a and b) are created; A and B: points equidistant from O ($d_A = d_B$) where the polarization of the entangled photons is measured.

(photons or gravitons). This means that classical physical phenomena are described by local models. Many physicists are unsatisfied of the non local character of *QM* and alternative local models have been proposed to explain quantum correlations. The simplest way to explain the non local aspects of *QM* as well as its probabilistic behaviour is to assume a lack of complete information about the actual state of the system in analogy with what happens for thermodynamic systems. Then, one could explain the probabilistic behaviour predicted by *QM* as due to a not complete knowledge of all influences affecting the system (*hidden variables*). In particular, the polarizations of the entangled photons a and b would be already well defined (by their hidden variables) when they are created at point O. However, as shown by Bell [2] and other authors [3, 4], the correlations between entangled particles predicted by any theory based on local hidden variables must satisfy some inequalities that are not satisfied by *QM*. The existence of these inequalities permits to perform experiments to decide unambiguously between hidden variables theories and *QM*. Many experiments of this kind have been performed before and after the famous Aspect experiments [5–14]. All the experiments (except a few old ones [15, 16], see cap. 11 of [17] for a detailed bibliography) demonstrated that the Bell inequalities are violated. Although the locality loophole and the detection loophole have not yet completely closed using a single experimental apparatus [18], experiments have separately closed both the locality loophole [6–10] and the detection loophole [12–14]. Then, it is reasonable to think that hidden variables alone cannot justify the experimentally observed correlations (except if implausible combinations of loopholes are supposed to exist). For many classical systems, correlations between two events are often explained as the consequence of communications and, thus, also quantum correlations between entangled particles could be due to some communication. However, the Aspect experiments and many other *EPR* experiments were performed in space-like conditions and, thus, if Quantum correlations would be due to communications, the communications velocity should exceed the light velocity c. For this reason, after the Aspect experiment, Bell said "*in these EPR experiments there is the suggestion that behind the scenes something is going faster than light*"[19]. Successively, well defined models for *QM* based on the presence of superluminal communications have been proposed [20, 21]. The possibility of the existence of particles going faster than light (*tachyons*) has been proposed some years ago by some authors [22–24]. Tachyons are known to lead to causal paradoxes [25] (the present occurring in a given point can be affected by the future occurring in the same point). Consider, for instance, a first person that exits from his home and is wetted by rain. He could send a tachyon to inform a second person that send a replay tachyon that is received by the first person before he exits from the home. Then, he could decide to get an umbrella to be not wetted by the rain. Obviously such a behaviour is unrealistic. However, no causal paradox arises if tachyons are supposed to propagate in a preferred frame where the tachyon velocity $v_t = \beta_t c$ ($\beta_t > 1$) is the same in all directions (see, for instance, [26–30]). Note that also in this case the Special Relativity predicts that a tachyon that is emitted at point A at the local time $t = 0$ can get point B at time $t < 0$. However, this does not represent a paradoxical result since the time ordering between separated points of the space has no direct physical meaning. Indeed, the time ordering between events occurring in different space points is conventional and depends on the conventional procedure used to synchronize far clocks. We assume here the conventionalist

thesis on the synchronization of distant clocks [31]. It is true that we cannot yet consider closed the debate on this topic [32], but we believe that the conventionalist thesis is the correct one.

Consider, now, two photons that are in the entangled state of Eq.(1) and suppose that photon a passes through a polarizing filter with horizontal polarization axis. According to the superluminal models of *QM*, when photon a passes through the polarizing filter, it collapses to the horizontally polarized state, then a tachyon is sent to the entangled photon b that collapses to the horizontally oriented state only after this communication has been received. Therefore, the *QM* correlations between entangled photons can be recovered only if it has been sufficient time to communicate between the two entangled photons. Consider, for instance, an ideal experiment performed in the tachyon preferred frame S' where two polarizing filters lie at points A and B at the same optical distances $d'_A = d'_B$ from source O of the entangled photons as shown in Fig.1. In these conditions photons a and b get both polarizers at the same time (in the *PF*) and, thus, if the tachyon velocity in the *PF* has a finite value, no communication is possible and correlations between entangled particles should differ appreciably from the predictions of *QM*. Of course, there is always communication if the tachyon velocity is $v_t \to \infty$, then no experiment satisfying *QM* can invalidate the superluminal models provided $v_t \to \infty$. In such a case superluminal models are completely equivalent to *QM* as occurs for the Bohm model [33, 34]. It has been recently shown [35, 36] that, if *QM* correlations are due to superluminal signals with finite velocity v_t, then superluminal signalling becomes possible, that is communications at faster than light velocity must be possible at a macroscopic level and they cannot be confined to "hidden" variables.

From the experimental point of view, equality $d'_A = d'_B$ can be only approximatively verified within a given uncertainty $\Delta d'$. Consequently, photons a and b could get the polarisers at two different times ($\Delta t' = {}^{\Delta d'}/_{c}$) and, thus, they could communicate only if the tachyon velocity exceeds a lower bound $v_{t,min} = {}^{d'_{AB}}/_{\Delta t'}$ where d'_{AB} is the distance between points A an B in the *PF*. The possible results of such an experiment are: *i)* a lack of quantum correlations is observed; *ii)* quantum correlations are always satisfied. In the first case (*i)*) one can conclude that orthodox *QM* is not correct and that quantum correlations are due to exchange of superluminal messages. By suitably changing distances d'_A and d'_B one could obtain a measure of the tachyon velocity v_t. In the second case (*ii)*), due to the experimental uncertainty, one cannot invalidate the tachyon model of *QM* but can only establish a lower bound $v_{t,min}$ for the tachyon velocity. So far we assumed that the experiment is carried out in the preferred frame, but velocity vector $\vec{V}$ of *PF* is unknown and, thus, the experiment cannot be performed in this frame. It will be shown in Section 2 that this drawback can be bypassed performing the experiment on the Earth with the *A*-*B* axis aligned along the West-East direction. Such an experiment could provide both the tachyon velocity v_t and the the velocity vector $\vec{V}$ of the *PF*.

A long-distance (10.6 km) *EPR* experiment to detect possible effects of superluminal quantum communications has been performed by Scarani et al. [37] using energy-time entangled photons. No deviation from the predictions of *QM* was observed and, thus, the authors obtained only a lower bound for the tachyon velocities in the *PF*. The experimental results were analyzed under the assumption that the preferred frame is the frame of cosmic microwave background radiation. With this assumption, the authors obtained a lower bound $v_{t,min} = 1.5 \times 10^4\, c$. Successively, similar long-distance measurements have been performed by Salart et al. [38] improving some features of the previous experiment and using detectors aligned close to West-East direction (at angle $\alpha = 5.8°$). The authors found a lower bound for the tachyon velocity for many different possible directions of velocity $\vec{V}$ of the *PF*. More recently [39] we performed *EPR* measurements on polarization entangled photons in a laboratory experiment with small distances $d_A \approx d_B \approx 1\,\mathrm{m}$ and with the *AB* axis in Fig.1 precisely aligned along the West-East direction ($|\alpha| < 0.2°$). In our experiment, too, no deviation from the predictions of *QM* was found and, thus, we obtained only a lower bound for the tachyon velocity. The choice of aligning

the measurement points A and B just along the West-East direction allowed us to obtain a lower bound for the tachyon velocity for any possible orientation of the velocity of the preferred frame. The experiment in [38] and in [39] are somewhat complementary. Indeed, the Salart et al. experiment used very large distances ($d_A \approx d_B \approx 10\,\mathrm{km}$) but somewhat large acquisition times ($\delta t \approx 360\,\mathrm{s}$), while our experiment used shorter distances ($d_A \approx d_B \approx 1\,\mathrm{m}$) but much shorter acquisition times ($\delta t \approx 4\,\mathrm{s}$). With these features, the Salart et al. experiment was much more sensitive to tachyons propagating in PF that have velocities much smaller than the light velocity whilst our experiment was more sensitive to PF travelling at higher velocities (see Fig.4). As will be shown in Section 2, an EPR experiment similar to our previous experiment but with entangled photons that propagate in air at much larger distances (of order of 1 km) and with much smaller acquisition times (of order of 0.1 s) could increase greatly the range of detectable tachyon velocities. To get this goal, we plan to perform such an experiment inside the long galleries of the EGO structure (European Gravitational Observatory) [40]. In this paper, we will analyse the main features of the proposed experiment. The possible results of this experiment are either the detection of possible discrepancies between experiment and QM due to a finite velocity superluminal communication or the increase by about two orders of magnitude of the actual lower bounds for the tachyon velocities.

The main features of the experiment are discussed in Section 2. The critical points and the main sources of experimental uncertainty are discussed in Section 3. Finally, the conclusions are given in Section 4.

2. The main features of the experimental method.

Consider the geometry of Fig.1. We start considering the ideal case where the experiment is performed in the preferred frame S' with tachyons that propagate with the same velocity $v_t = \beta_t c$ ($\beta_t > 1$) along any direction [38]. For simplicity, in the following, we will call "tachyon velocity" the reduced velocity $\beta_t = \frac{v_t}{c}$. Two polarizing filters lie at points A and B aligned along a x'-axis and at optical distances d'_A and d'_B from the source O of the entangled photons (the apostrophe denotes the parameters measured in the PF). The two entangled photons will get both the polarisers at the same times $t'_A = t'_B$ if $d'_A = d'_B$ and, thus, no superluminal communication can be possible if the tachyon velocity has a finite value. Due to the experimental uncertainty $\Delta d'$, distances d'_A and d'_B can never be exactly equalized and $|\Delta t'| = |t'_A - t'_B| = {}^{\Delta d'}/_{c} \neq 0$. In these conditions, a superluminal communication between points A and B will be not possible only if the time that a tachyon spend to go from A to B (or from B to A) is greater than $|\Delta t'|$, that is if the tachyon velocity β_t is smaller than

$$\beta_{t,min} = \frac{d'_{AB}}{|\Delta c t'|}, \tag{2}$$

where d'_{AB} is the distance between points A and B. QM correlations will be always established if the tachyon velocity β_t is higher than $\beta_{t,min}$ of Eq.(2) but appreciable differences between QM correlations and experimentally observed correlations is expected if $\beta_t < \beta_{t,min}$. In this latter case, the experimental correlations should satisfy the Bell inequality. Therefore, to detect possible discrepancies between experiment and QM due to the finite velocity of tachyons, one has to increase the lower limit in Eq.(2) as much as possible to satisfy condition $\beta_t < \beta_{t,min}$. This goal could be achieved either reducing $\Delta d' = |\Delta c t'|$ or increasing distance d'_{AB} between the polarisers. If discrepancies between QM and experiment would be found for given values of $\Delta d'$ and d'_{AB}, one could conclude that the tachyon velocity is lower than the lower bound in Eq.(2). In such a case, one could measure the tachyon velocity β_t changing distances d'_A, d'_B and d'_{AB} to reduce $\beta_{t,min}$ of Eq.(2) until condition $\beta_{t,min} < \beta_t$ is verified and QM correlations are re-established. The tachyon velocity β_t would correspond to this critical value of $\beta_{t,min}$.

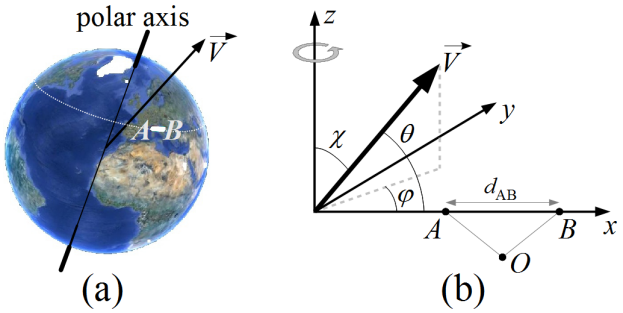

Figure 2: (a) geometry of the experiment with segment AB oriented along the West-East direction on the Earth; (b) detail of the geometric parameters that characterize the experiment. z is the North-South axis and x is the West-East axis. $\vec{V}$ is the velocity vector of the PF with respect to the laboratory, θ denotes the angle of $\vec{V}$ with the x-axis, φ is the azimuthal angle and χ is the polar angle. The polarizing filters that collect the entangled photons lie at points A and B aligned along the x-axis at the same optical distances from the source O of the entangled photons.

The results above were obtained assuming that the experiment is performed in the tachyons PF. Of course, this is not possible because we do not know what is the direction and the magnitude of the PF velocity $\vec{V} = \vec{\beta}c$. However, this apparent difficulty can be overcome if one takes advantage of the rotation motion of the Earth around its axis and aligns points A and B along the West-East x-axis on the Earth as shown in Fig.2. Suppose that points A and B are precisely aligned along the x-axis and that optical distances d_A and d_B of A and B from the entangled photon source O have the same values on the Earth frame. In this condition, the two entangled photons get the two polarizing filters at the same times t_A and t_B in the Earth frame but the arrival times t'_A and t'_B can be different in the tachyon PF. Due to the rotation of the Earth with the angular velocity ω, angle θ between the the velocity $\vec{V}$ of the PF and the x-axis (West-East direction) changes periodically with time t according to the simple law:

$$\theta(t) = \arccos\left[\sin\chi\cos\omega\,(t - t_0)\right], \tag{3}$$

where t_0 is the unknown time which gives $\varphi\,(t) = 0$ in Fig.2. Angle θ oscillates periodically between a minimum value $\pi/2 - \chi$ ($\varphi(t)$=0 in Fig.2) and a maximum value $\pi/2 + \chi$ ($\varphi(t)$=π in Fig.2). Then, whatever is the orientation of the velocity vector $\vec{V}$ of the PF, there are two times t_1 and t_2 during each sidereal day where $\vec{V}$ becomes perpendicular to the West-East x-axis. At these two times, according to the Special Relativity, the distances of A and B from O are equal also in the PF frame ($d'_A = d'_B$) and, thus, the arrival of the entangled photons at points A and B is simultaneous also in the PF. Then, deviations of correlations from the predictions of the QM should be observed at the special times t_1 and t_2 if the optical paths of the entangled photons would be equal. Of course, due to the experimental uncertainty Δd on the equalization of the optical paths, deviations from the predictions of QM could be only observed if the tachyon velocity β_t is lower than a lower bound $\beta_{t,min}$. Furthermore, the need of performing the experiment in the Earth frame introduces also another source of uncertainty because vector $\vec{V}$ becomes orthogonal to the West-East axis only at two well defined times t_1 and t_2. However, to detect a statistically significant number of coincidences of entangled photons, a sufficiently long acquisition time δt is needed. Also if this acquisition time is centred around the special times t_1 and t_2, the velocity vector $\vec{V}$ does not remain exactly perpendicular to the x-axis during the whole acquisition time. Therefore, the finite acquisition time leads to an adjunctive uncertainty on the equality of the optical paths with a consequent decreasing of the value of $\beta_{t,min}$. In conclusion, two main parameters determine the lower limit of $\beta_{t,min}$ obtainable with

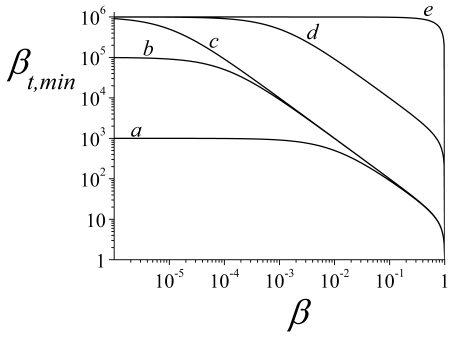

Figure 3: The typical plot of function $\beta_{t,min}$ versus β is shown for the unfavourable case $\chi = \pi/2$ and for some values of the experimental parameters $\bar{\rho}$ and δt. Curves a, b and c correspond to the fixed acquisition time $\delta t = 10^{-1} \times \frac{T}{\pi}$ and to decreasing values of $\bar{\rho}$ ($a : \bar{\rho} = 10^{-3}$, $b : \bar{\rho} = 10^{-5}$, $c : \bar{\rho} = 10^{-6}$). Curves c, d and e correspond to a fixed value $\bar{\rho} = 10^{-6}$ and to decreasing values of δt ($c : \delta t = 10^{-1} \times \frac{T}{\pi}$, $d : \delta t = 10^{-3} \times \frac{T}{\pi}$, $e : \delta t = 10^{-7} \times \frac{T}{\pi}$). Note that curve e satisfies condition (7) and, thus, it depends on β only for PF moving at improbable relativistic velocities.

the measurements on the Earth frame: 1) the accuracy Δd on the equalization of the optical paths; 2) the finite acquisition time δt. The lower bound $\beta_{t,min}$, defined by Eq.(2), can be rewritten in terms of physical parameters measured in the Earth frame and becomes [38, 39]:

$$\beta_{t,min} = \sqrt{1 + \frac{(1-\beta^2)\,[1-\bar{\rho}^2]}{\left[\bar{\rho} + \beta \sin\chi \sin\frac{\pi\delta t}{T}\right]^2}}, \tag{4}$$

where $\bar{\rho} = \frac{\Delta d}{d_{AB}}$, T is the sidereal day, δt is the acquisition time, χ is the polar angle between the North-South axis of the Earth and velocity $\vec{V}$ of the PF (see Fig.2) and β is the reduced velocity ($\beta = V/c$) of the PF. A quick way to obtain (4) is shown in the Appendix. In typical experimental conditions [38, 39], the acquisition time δt is much smaller than the sidereal day T and $\beta_{t,min}$ is a decreasing function of both $\bar{\rho}$ and δt and reaches a minimum value if $\chi = \pi/2$. Our following considerations and figures will be restricted to $\delta t \ll T$ and to the unfavourable condition $\chi = \pi/2$. $\beta_{t,min}$ is also a decreasing function of β that assumes its maximum value $\beta_{t,min} = \frac{1}{\bar{\rho}}$ for $\beta = 0$ and approaches the minimum value $\beta_{t,min} = 1$ for $\beta \to 1$. The typical plot of function $\beta_{t,min}$ versus the reduced velocity β of the PF for $\chi = \pi/2$ is drawn in Fig.3 for some values of the experimental parameters $\bar{\rho}$ and δt. $\beta_{t,min}$ keeps an almost constant value $\beta_{t,min} \approx \frac{1}{\bar{\rho}}$ for $\beta \ll \beta_0 = \bar{\rho}T/(\pi\delta t)$, then it decreases rapidly as β increases above β_0. Eq.(4) and Fig.3 evidence what is the optimal strategy to increase $\beta_{t,min}$ as much as possible. First of all we must reduce $\bar{\rho}$ minimizing the uncertainty Δd and increasing distance d_{AB} as far as possible. Then, we must use an acquisition time δt sufficiently small to render negligible the δt-contribution in Eq.(4). This contribution is always negligible if:

$$\delta t \ll \bar{\rho}\frac{T}{\pi}. \tag{5}$$

If condition (5) is satisfied, the lower limit $\beta_{t,min}$ becomes insensitive to the acquisition time δt.

In the Geneva experiment [38] the very small value $\bar{\rho} = 5.4 \times 10^{-6}$ was obtained using Telecom optical fibres connecting two Telecom stations at a distance of about 20 km and aligned approximatively along the West-East direction. The experiment was performed using energy-time entangled photons. The two Telecom stations (A and B) were not exactly aligned along the West-East axis but did the angle $\gamma = 5.8°$ with this axis and, thus, the experiment was poorly sensitive to tachyons PF travelling with velocity $\vec{V}$ lying in a cone of aperture $\approx 6°$ around the North south axis. Indeed, due to the Earth rotation, the angle between the AB axis and the velocity vector $\vec{V}$ oscillates with time between the minimum value $\pi/2 - \chi - \gamma$ and the maximum value $\pi/2 + \chi - \gamma$. Then, the AB axis can become orthogonal to $\vec{V}$ only if $\chi \geq \gamma$. In this long path experiment the main effect that limited a further reduction of $\bar{\rho}$ was due to the appreciable optical dispersion of the photon wave-packet in the long Telecom fibres. On the other hand, due to losses in the optical fibres, the photons count rate was relatively

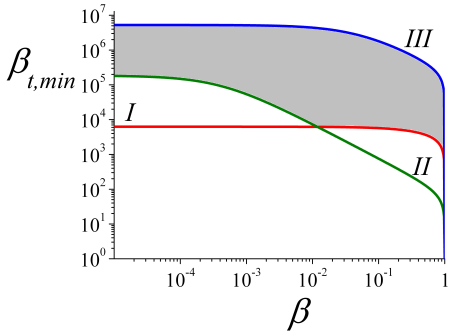

Figure 4: The three curves *I* (red), *II* (green) and *III* (blue) correspond to the experimental results for the lower bound $\beta_{t,min}$ versus β in different experiments. *I*: our previous results ($\bar{\rho} = 1.6 \times 10^{-4}$, $\delta t = 4$s) ; *II*: the Geneva group results ($\bar{\rho} = 5.4 \times 10^{-6}$, $\delta t = 360$s) ; *III*: the predicted results for the experiment proposed here ($\bar{\rho} = 1.9 \times 10^{-7}$, $\delta t = 0.1$s). The gray region represents the new region of tachyons velocities β_t that would become accessible with the new experiment.

small and a somewhat long measurement time ($\delta t \approx 360$ s) was needed to obtain a statistically significant number of coincidences. In these conditions the experiment was greatly sensitive to tachyons *PF* travelling at speeds much smaller than that the light velocity and much less sensitive to relativistic *PF* (see curve *II* in Fig.4). The Pisa experiment [39] was performed with entangled photons that propagate in air over much shorter distances (about 2 m) and the polarization correlations were measured instead of energy-time correlations. In these conditions photon losses were minimized and the typical acquisition time was $\delta t \approx 4$ s. An interferometric method was used to minimize the uncertainty on the equalization of the photons optical paths and the main source of uncertainty Δd was due to the 220 μm thickness of the absorbing layer of the polarizing filters. The obtained value of parameter $\bar{\rho}$ was $\bar{\rho} = 1.6 \times 10^{-4}$ that is about 30 times higher than the value characterizing the experiment of [38]. Then, our experiment is much less sensitive than that in [38] to tachyons propagating in a low speed *PF* but is more sensitive to tachyons propagating in high speed *PF* (see curve *I* in Fig.4). In this sense, our experiment was somewhat complementary to that of the Geneva Group. In the present paper we propose a new experiment exploiting the propagation of polarized entangled photons in air at distances about 850 times longer than in our previous experiment. The experiment should be performed inside the long tunnels of the European Gravitational Observatory (*EGO*) that host the *VIRGO* experiment on the detection of gravitational waves [41]. Using an interferometric method and feedback procedures we will hold the uncertainty Δd on the equality of the optical paths of the entangled photons well below the basic uncertainty due to the thickness of the absorbing layer of the polarizing filters (220 μm). The small uncertainty and the long optical paths will allow us to decrease our previous value $\bar{\rho} = 1.6 \times 10^{-4}$ up to the much smaller value $\bar{\rho} = 1.9 \times 10^{-7}$. As shown in the discussion above, the lower bound for the tachyon velocities is also determined by the acquisition time δt that must satisfy the condition that the number of detected coincidences must be statistically relevant. δt can be reduced increasing the brightness of the source of the entangled photons and minimizing the losses. In some papers, the Kwiat group [42–44] developed a very efficient and simple method to obtain highly bright sources of entangled photons with a high degree of entanglement. Using this technique and a suitable optical configuration we plan to increase by more than 1000 times the number of measured coincidences and to reduce the acquisition time to less than $\delta t = 0.1$ s. The lower bounds obtained in the previous experiments together with the new lower bound that should be reached with the experiment proposed here are shown in Fig.4. Curve *I* (red) corresponds to our previous experimental results, curve *II* (green) to the results of the Geneva group and curve *III* (blue) to the results expected with the proposed experiment. The grey region corresponds to the new region of tachyon velocities that could become accessible.

In the next section, the critical points of the proposed experiment and the main sources of experimental uncertainty will be discussed.

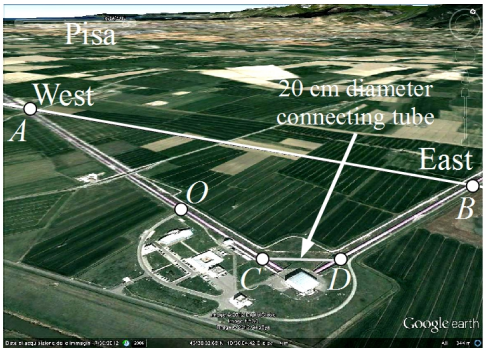

Figure 5: A Google earth view of the *EGO* structure with the two orthogonal tunnels is shown together with the West-East line. Point O represents the position of the source of entangled photons, while A and B denote the positions of the two polarizing filters in the two *EGO* arms. The full line represents the West-East direction. The entangled photon that travel at the right of point O will be deviated from the tunnel containing source O to the other tunnel passing through a suitable CD tube (20 cm diameter) that will be built to connect the two arms of the *EGO* structure.

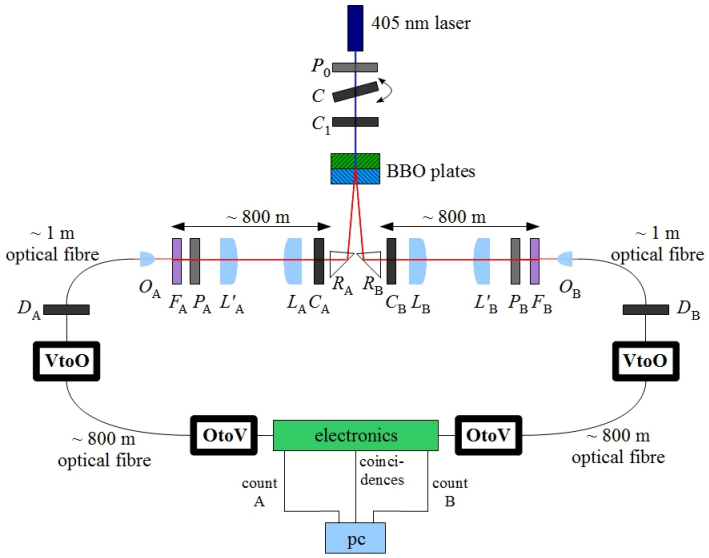

Figure 6: Schematic view of the experimental apparatus. To simplify the drawing, the optical path followed by the left entangled photon has been represented by a straight line and the optical prisms that deviate the beam from a tunnel to the other (see Fig.5) are not shown. A 405 nm laser beam impinges on two adjacent *BBO* plates with orthogonal optical axes and produces two 810 nm entangled beams preferentially emitted at the symmetric angles $\alpha_A = -\alpha_B \approx 2°$. C, C_1, C_A and C_B are optical compensators, R_A and R_B are two right angle prisms; L_A, L'_A, L_B, L'_B are large diameter (18 cm) planoconvex lenses, P_A and P_B are polarizing filters that are at the same distance from source O, F_A and F_B are optical interferometric filters with 10 nm line-width, O_A and O_B are aspheric lenses and D_A and D_B are single photons counters. $V\text{to}O$ and $O\text{to}V$ are voltage pulses to optical pulses converters and vice-versa.

3. The experiment: critical points and main sources of experimental uncertainty

As stated above, the polarizing filters should be aligned along the West-East direction, but the *EGO* tunnels are oriented at 19° and 109° with respect to this direction, respectively. Therefore, the polarizing filters must be placed in two different tunnels and one of the entangled photons must be deviated from a *EGO* tunnel to the other through the small CD tube (20 cm diameter, 100 m length) built to connect them. The source of the entangled photons (point O) will be placed in the 19° tunnel together with polariser P_A at distance $\approx$ 800 m while polariser P_B will be placed at point B in the other *EGO* tunnel at the same distance from O as shown schematically in Fig.5 ($\overline{OA} = \overline{OC} + \overline{CD} + \overline{DB}$).

The experimental apparatus is schematically shown in Fig.6 where, for simplicity of drawing, the path $OCDB$ shown in Fig.5 has been represented by a straight line and the prisms needed

to deviate the photons from one *EGO* arm to the other are not represented. A blue diode laser beam ($\lambda = 405\,\mathrm{nm}$) is polarized at 45° with respect to the vertical axis by polariser P_0, passes through a tilting plate optical compensator (C) with vertical extraordinary axis and the quartz compensator (C_1) with horizontal extraordinary axis and, finally, impinges at normal incidence on two thin (0.5 mm) adjacent non-linear optical crystals (BBO) cut for type-I phase matching [45]. The optic axes of the adjacent BBO crystals are tilted at the angle 29.2° and lie in planes perpendicular to each other with the first plane that is horizontal. The pump beam induces down conversion at $\lambda = 810\,\mathrm{nm}$ in each crystal [45] with a maximum of emission at the two symmetric angles $\alpha_A = -\alpha_B \approx 2°$ with respect to the pump laser beam. The down converted photons are created in the maximally entangled state $\left(|H, H> + e^{i\phi}|V, V>\right)/\sqrt{2}$, where phase ϕ can be adjusted tilting the optical compensator C. R_A and R_B are two right angle prisms, C_A and C_B are optical BBO plates with tilt angle 29.2°, P_A and P_B are thin near infrared polarizing films (LPNIR, Thorlabs), F_A and F_B are interference filters ($\lambda = 810\,\mathrm{nm} \pm 5\,\mathrm{nm}$) and D_A and D_B are single photons counters (Perkin Elmer SPCM-AQ4C). L_A, L_B, L'_A and L'_B are large plano-convex optical lenses (18 cm-diameter) that ensure that all the entangled photons emitted within a cone of $\approx 0.35°$ aperture angle (around the two maximum emission directions $\alpha_A = -\alpha_B \approx 2°$) can be collected by aspheric objectives O_A and O_B and sent to detectors D_A and D_B. The centres of polarisers P_A and P_B are aligned along a x-axis in the West-East direction within $\approx 0.1°$. The role of P_0, C, P_A, P_B, F_A and F_B is shown in [45]; the role of C_1, C_A and C_B is explained in [42–44] and is resumed in Section 3.1. The outputs electric pulses of the detectors (20 ns width) are transformed into optical pulses, sent via optical fibres to the central region close to the photon source, transformed again to electric pulses and sent to electronic counters and to a coincidence circuit connected to a PC. A labview program controls any experimental feature.

The results shown in curve *III* of Fig.4 were obtained assuming that the uncertainty Δd can be maintained much lower than the thickness of the polarizing layers ($\approx 220\,\mu\mathrm{m}$) and the acquisition time can be small enough ($\delta t \approx 0.1\,\mathrm{s}$). Here below we will describe how both these conditions can be satisfied.

3.1. Minimization of the acquisition time δt.

The minimum acquisition time δt is determined by the condition that the number of detected entangled photons must be statistically significant during time δt (> 1000 measured coincidences). Then, low values of δt can be obtained only if: *a*) the number of entangled photons collected by lenses L_A and L_B is large enough, *b*) the losses of the entangled photons in the path from the source to the detectors are as smaller as possible. The momentum conservation would require that the entangled photons are emitted at two well defined angles ($\alpha_A = -\alpha_B \approx 2°$), but, due to the finite thickness of the BBO plates (0.5 mm), a $\approx \pm 0.35°$ spreading around these directions occurs. Then, a large fraction of the entangled photons can be collected only if the aperture angle of lenses L_A and L_B with respect to the photon source is $\approx 0.35°$. However, due to the great optical anisotropy of the BBO plates, the relative phase between entangled photons (ϕ in Eq.(1)) depends greatly on the emission direction. This means that the entanglement of the photons is satisfactory (close to 100% fidelity) only if the aperture angle is $\ll 0.05°$. Furthermore, the number of entangled photons greatly increases with the power of the pump laser diode and, thus, a high power laser diode should be used. However, high power laser diodes (> 50 mW) are characterized by a small coherence length which is typically $\approx 0.2\,\mathrm{mm}$. In these conditions, the V-polarized down converted photons that are produced in the first BBO plate (0.5 mm thick) are essentially uncorrelated with respect to the H-polarized photons produced in the second adjacent plate and, thus, the entanglement is very poor. This latter drawback could be avoided using high coherence length laser diodes but, in this case, the laser power would be smaller than 50 mW. The Kwiat group [42–44] showed that the drawbacks described above

can be bypassed using suitable optical compensators (C_1, C_A and C_B in Fig.6). C_1 is a quartz plate that introduces a retardation between the V and the H components of the pump beam virtually equal to the difference between the emission times of down converted photons from the two BBO plates. In this way, the losses of entanglement due to the low coherence of the laser beam are virtually eliminated. C_A and C_B are two anisotropic plates (BBO) with a suitable thickness to compensate the phase differences between entangled photons propagating along different directions. Using these compensation methods with a 280 mW laser beam and collecting entangled photons with a 0.35° aperture angle, the Kwiat group obtained an ultra bright and high fidelity (99 %) source of entangled photons with 1.02×10^6 detected coincidences/s. In our experiment we require also that all the entangled photons that are emitted within the 0.35° aperture angle get photodetectors D_A and D_B at a great distance (≈ 800 m) from the source. Furthermore, it is convenient to maintain the diameter of the entangled beam sufficiently smaller when passes through the 20 cm-diameter connecting tube. Both these conditions are satisfied using large diameter (18 cm) plano-convex lenses with long focal length $f = 10$ m and slightly focusing the pump beam on the BBO plates to have a source of entangled photons with a small diameter D ($D \lesssim 0.5$ mm). Lenses L_A and L_B are put at a distance from the source slightly higher than f to produce real images of the source approximatively at distance $d_i \approx 400$ m from L_A and L_B. In this condition, the image produced by lens L_B occurs in the centre of the connecting tube. The image diameter is $D_i \approx D\ {}^{d_i}/_{f}$ =2 cm that is much smaller than the 20 cm-diameter of the connecting tube. Furthermore, due to the large diameter of lenses, the enlargement produced by diffraction is negligible. In these conditions all the entangled photons emitted in the cones of aperture angle 0.35° are collected by the large diameter lenses L_A, L'_A and L_B, L'_B and real images of the source with diameter $D'_i \approx D = 0.5$ mm are generated on the surfaces of polarisers P_A and P_B at distance slightly higher than $f = 10$ m from lenses L'_A and L'_B. The optical rays exiting from these images are collected by the aspheric objectives O_A and O_B that focus the entangled photons on two 60 μm-diameter optical fibres connected to detectors D_A and D_B. Using the Zemax optical design program we have verified that this geometric arrangement ensures that all the entangled photons emitted by the source within the 0.35° aperture angle are collected by detectors.

The previous analysis was performed disregarding any effect due to the presence of air. Density fluctuations of air produce wander of the photons beams and beam size variations that could reduce our collection efficiency. To estimate the relevance of these effects we consider the experimental results obtained by Resch et al. [46] that performed measurements with entangled photons propagating between two buildings on the Vienna sky at a distance of 7.8 km. Due to air turbulences, the authors observed large beam size variations (displacement of the centre of the beam and changes of diameter) of about 25 cm at distance 7.8 km from the source. Making a linear extrapolation of the Resch et al. results to our experimental lengths (≈ 0.8 km $\ll 7.8$ km), we expect that beam size variations should be reduced to less than 2.6 cm in our experiment. The diameter of lenses L'_A and L'_B is 18 cm whilst the diameter of entangled beams impinging on lenses L'_A and L'_B is expected to be < 14 cm, then, the 2.6 cm displacements should not affect appreciably the collection efficiency.

Another effect that could reduce the collection efficiency is the air absorption at the wavelengths of the entangled photons ($\lambda = 810$ nm $\pm$ 5 nm). However, air is known to exhibit a transmission window at these frequencies (see Fig.8 in [47]) and, thus, losses due to absorption are expected to be not dramatic. Precise in loco measurements would be needed to evaluate losses due to absorption. However, one can obtain a very rough upper estimate of the losses due to absorption yet using the results by Resch et al. obtained with 810 nm entangled photons propagating on the Vienna sky. In their experiment with the 7.8 km distance they observed that only a 1.4% fraction of the photons emitted by the source actually reached the detectors at the 7.8 km distance. Note that the average beam displacements in their experiment were very large

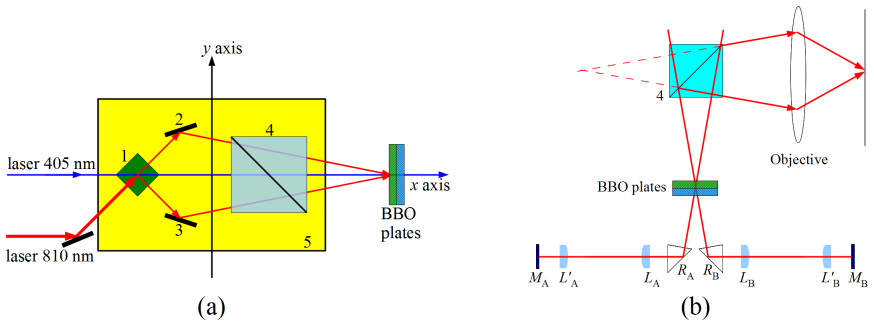

Figure 7: (a): system used to obtain two laser beams impinging at $\pm 2°$. 1 and 4 are beam splitters, 2,3 are mirrors and 5 is a rigid plate that is mounted on a x-y carriage that allows its insertion and removal. Beam splitter 4 needs to collect the beams reflected by mirrors M_A and M_B as shown in Fig.(b). (b): A schematic view of the interferometer. The laser beams are reflected by mirrors M_A and M_B, go back and produce a interference pattern in the surface corresponding to the central plane of the BBO plate. Then, beams are reflected by beam splitter 4 and a magnified image of the interference pattern is produced by the objective.

(25 cm) and greater than the diameter of their collecting telescopes. Then, beam displacements are expected to appreciably reduce the photon counts in their experiment. However, also assuming that losses would be entirely due to absorption, one would obtain the absorption coefficient $\alpha = 5.5 \times 10^{-4}\,\mathrm{m}^{-1}$ that would correspond to a 65% collection efficiency for a beam that propagates at a 800 m distance. Tacking into account for the entangled photon intensities reported in [46], we can conclude that, using a 120 mW laser diode and using suitable compensation procedures and a proper optical design, the number of measured coincidences should be $\gg 10^5$ coincidences/s that is more than 10^4 coincidences during the acquisition time $\delta t = 0.1\,\mathrm{s}$.

3.2. Equalization of the optical paths.
The optical apparatus in Fig.6 provides the collection of a large number of entangled photons (99%-fidelity) emitted within the 0.35° aperture angle during the short acquisition time $\delta t = 0.1\,\mathrm{s}$. However, a high value of the lower bound $\beta_{t,min}$ can be obtained only if also parameter $\bar{\rho}$ has a very small value, that is if the uncertainty on the equalization of the optical paths OA and OB is small enough. In our experiment, the thickness of the sensitive layer of the polarizing filters is $220\,\mu$m and this leads to an intrinsic uncertainty $\Delta d \lesssim 220\,\mu$m, that defines the minimum obtainable value of $\bar{\rho}$ in Eq.(4). Then, it is sufficient to require that the difference between the optical paths of the entangled photons is much smaller than $\Delta d \lesssim 220\,\mu$m. This goal will be reached using the interferometric method described below. Initially, polarisers P_A and P_B will be positioned approximatively at the same distance (within one centimeter) using GPS and, successively, the distances will be equalized with the interferometric method with an estimated accuracy better that $10\,\mu$m.

To obtain the paths equalization, we will use a 810 nm laser diode with low coherence length ($0.1 - 0.2\,\mathrm{mm}$). Using the simple optical system in Fig.7(a), we will obtain two beams that impinge with equal phases on the central point of the BBO plates with incidence angles $\pm 2°$. In such a way the outgoing beams follow the same paths of the entangled beams. Then, the BBO plates will be removed using a translator and polarisers P_A and P_B will be replaced by two mirrors M_A and M_B. The laser beams reflected by mirrors M_A and M_B will go back and will again meet the position of the central plane of the BBO plates (now removed) where they form an interference pattern with a $\approx 10\,\mu$m interline. The transmitted beams will be collected by beam splitter 4 in Fig.7(b) and a magnified image of fringes will be produced by

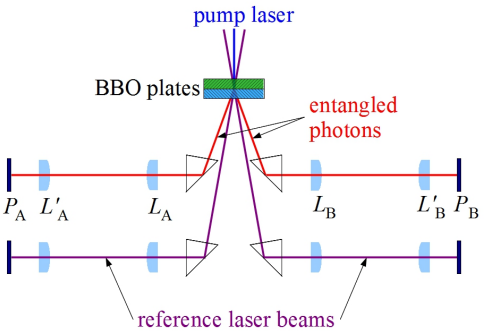

Figure 8: Schematic view of the paths of the entangled photons and of the reference laser beams.

the objective. Fringes will be visible only if the difference of optical paths is lower than the coherence length of the laser beam ($0.1 - 0.2$ mm) with a maximum visibility when the optical paths are equalized. Translating one of the mirrors with a motorized micrometer carriage and doing real-time measurements of the fringes visibility, the optical paths can be equalized within $\pm 10\,\mu$m (for a detailed analysis see [39]). Satisfactory preliminary tests of the proposed optical scheme have been carried out in our laboratory over distances of about 10 m. Once the optical paths are equalized, mirrors M_A and M_B should be replaced by polarizes P_A and P_B, using the procedures described in [39] that ensure that the surfaces of the polarizing layers just coincide with those of the mirrors within $\pm 10\,\mu$m.

The above procedure to equalize the optical paths leads to a satisfactory equalization (within $\pm 10\,\mu$m) at a given time. However, due to the long optical paths characterizing our experiment, temperature variations of the air refractive index can produce the optical paths variation:

$$\Delta L_{ott} = \left(\frac{\partial n^*}{\partial T}\right) L_0 \Delta T, \tag{6}$$

where L_0 is the initial path length, n^* is the group refractive index of air at the wavelength $\lambda = 810$ nm, $\partial n^*/\partial T = 9.47 \times 10^{-7}\,\mathrm{K}^{-1}$ [48] and ΔT is the difference between the mean temperatures along the paths of the two entangled photons. Substituting the path length value $L_0 = 800$ m in Eq.(6), we get $\Delta L_{ott} = 0.76$ mm for $\Delta T = 1^\circ$ C. Other contributions are expected from changes of air pressure and humidity, from thermal expansion and from Earth tides. The resulting expected variations of the optical paths are much greater than the accuracy required on the equalization of the optical paths. Then, a suitable feedback procedure to keep constant the paths difference is needed. To reach this goal, polariser P_B will be placed on a carriage driven by an electric motor and a proper feedback voltage will be sent to the electric motor. To obtain the feedback signal we want to build an interferometer with reference laser beams ($\lambda \approx 780$ nm) moving along the arms on paths parallel to those of the entangled photons but spatially separated at an average distance of $20 - 30$ cm (see Fig.8). Since the paths are sufficiently close, we think that the optical paths variations due to the above effects are similar for the entangled photons and for the reference beams. If this assumption is correct, one can measure the paths variations of the reference beams to obtain a feedback signal to translate the P_B polariser. Of course, the validity of this assumption has to be firstly checked. If the assumption would not be verified, it would be needed to use more complex feedback schemes as, for example, those used in [49] where the reference beams follow the same paths of the entangled photons. Finally, due to the long optical paths, a special care has to be devoted to take under control the laser beam pointing and possible drifts of the entangled beams trajectories.

4. Conclusions

In this paper, we propose a long distance *EPR* experiment performed exploiting the long paths that characterize the *EGO* structures to test the superluminal models of *QM*. Such an experiment should increase by about two orders of magnitude the actual lower bounds for the tachyon velocities. This goal can be reached using special compensation methods to obtain high intensity sources of entangled photons and interferometric methods to minimize the uncertainty on the optical paths. An important feature of this experiment is that the measuring points A and B are exactly aligned along the West-East axis. This alignment ensures that the experimental apparatus is sensitive to any possible orientation of the velocity vector of the preferred frame of tachyons. Therefore, if the Quantum Mechanic correlations between entangled photons would be entirely or partially due to superluminal communications and if the tachyon velocity in the *PF* would be lower than the $\beta_{t,min}$ value shown in the curve *III* in Fig.4, the measured correlations should exhibit appreciable deviations from the predictions of *QM*. In such a latter case, also the actual velocity of tachyons and the actual velocity of the *PF* could be obtained from further experimental measurements. If no deviation from the predictions of *QM* would be found, our experiment would provide a lower bound for the tachyon velocities two orders of magnitude higher than the actual ones. In our previous laboratory experiment [39] we tested only the simplest model of superluminal quantum communications where all correlations between entangled photons are only due to superluminal communications and no correlation exists if there is no communication. In such a special case, the model can be tested orienting the polarizing axes of polarisers P_A and P_B both at a $\pi/4$ angle with respect to the horizontal direction [H in Eq.(1)] and measuring the coincidences between photons passing through both the polarisers. However, according to Eberhard [20], this is only one of the possible superluminal models but more complex models are also possible. In particular, some correlation between entangled particles could be already present at the beginning (hidden variables) and only a part of quantum correlations could be due to superluminal communications. In such a case, also if particles have not sufficient time to communicate, some correlations between entangled particles remain. According to the Bell theorem, correlations due to hidden variables alone cannot reproduce entirely *QM* correlations and, in particular, they have to satisfy the Bell inequalities. Then, a general test of any kind of possible superluminal model can be made only measuring a Bell-like inequality. The Bell inequalities and other equivalent inequalities proposed in the literature, need measurements of coincidences between entangled photons passing through polarisers P_A and P_B for at least four different orientations of their axes. In our experiment, one channel polarisers (polarizing filters) are used and special B.C.H.S.H. inequalities must be considered [50]. In particular, for any hidden variables model, it has been shown that the quantity:

$$M = \frac{N(a,b) - N(a,b') + N(a',b) + N(a',b') - N(a',\infty) - N(\infty,b)}{N(\infty,\infty)} \tag{7}$$

must satisfy the inequality

$$-1 \leq M \leq 0. \tag{8}$$

N represents the number of measured coincidences between photons passing through polarisers P_A and P_B for some different orientations of the polarisers. a and a' are two different orientations of polariser P_A, b and b' are two different orientations of polariser P_B and symbol ∞ corresponds to a removed polariser. The maximum deviation of *QM* correlations from condition (8) occurs if the polarization directions a, a', b and b' are represented by angles $\theta_a = 0°, \theta_{a'} = 45°, \theta_b = 22.5°$ and $\theta_b = 67.5°$ with respect to the vertical axis. With this choice, a positive value of M is predicted by *QM* in disagreement with inequality (8).

From Eq.(7) we see that 7 different measurements of coincidences have to be performed to verify inequality (8). The measurements will be performed in this way: polarisers P_A and P_B

will be oriented along the first combination (a,b) occurring in Eq.(7) and coincidences will be detected during an entire sidereal day, then the polarisers orientations will be changed to the second combination (a,b') and measurements will be repeated until all the seven combinations have been considered. Finally, the value of quantity M at the different sidereal times t will be obtained substituting in Eq.(7) the coincidences measured at the same sidereal times of different sidereal days. In such a way, our experiment will provide a complete test of any possible model of QM superluminal communications.

Appendix

The Alice (A) and Bob (B) polarization measurements will be represented by the space-time events $(\vec{x}_A, ct_A)$, $(\vec{x}_B, ct_B)$ in the laboratory frame R and by $(\vec{x}'_A, ct'_A)$, $(\vec{x}'_B, ct'_B)$ in the tachyons preferred frame R', respectively. The invariance of the space-time intervals writes

$$(d_{AB})^2 - (\Delta ct)^2 = \left(d'_{AB}\right)^2 - \left(\Delta ct'\right)^2 \tag{A.1}$$

where $d_{AB} = |\Delta\vec{x}|$, with $\Delta\vec{x} = \vec{x}_B - \vec{x}_A$, $\Delta ct = ct_B - ct_A$, $d'_{AB} = |\vec{x}'_B - \vec{x}'_A|$ and $\Delta ct' = ct'_B - ct'_A$. Dividing both sides of Eq.(A.1) by $\left(\Delta ct'\right)^2$ we get

$$\left(\frac{d'_{AB}}{\Delta ct'}\right)^2 = 1 + \frac{d_{AB}^2 - (\Delta ct)^2}{\left(\Delta ct'\right)^2}, \tag{A.2}$$

where $\Delta ct'$ satisfies the Lorentz equation:

$$\Delta ct' = \gamma\left(\Delta ct - \vec{\beta}\cdot\Delta\vec{x}\right), \tag{A.3}$$

with $\vec{\beta} = \vec{V}/c$ ($\vec{V}$ is the velocity of R' with respect to R) and $\gamma = 1/\sqrt{1-\beta^2}$. Substituting $\Delta ct'$ of Eq.(A.3) in the right-hand side of Eq.(A.2) we obtain

$$\left(\frac{d'_{AB}}{\Delta ct'}\right)^2 = 1 + \frac{\left(1-\beta^2\right)\left[1 - \left(\frac{\Delta ct}{d_{AB}}\right)^2\right]}{\left(\frac{\Delta ct - \vec{\beta}\cdot\Delta\vec{x}}{d_{AB}}\right)^2}. \tag{A.4}$$

If $v_t = \beta_t c$ is the tachyons velocity in R', the quantum communication cannot occur (the Bell inequalities are verified) only if

$$\beta_t < \frac{d'_{AB}}{|\Delta ct'|}. \tag{A.5}$$

Inequality (A.5) would be always verified for any finite β_t provided the two conditions

$$\Delta ct = 0 \quad \wedge \quad \vec{\beta}\cdot\Delta\vec{x} = 0 \tag{A.6}$$

would be satisfied that lead to $\frac{d'_{AB}}{|\Delta ct'|} \to \infty$ in Eq.(A.4). However, due to the experimental features, conditions (A.6) can be only approximatively satisfied and, thus, discrepancies with the QM will occur only if

$$\beta_t < \beta_{t,min}, \tag{A.7}$$

where $\beta_{t,min}$ is the minimum value of $\frac{d'_{AB}}{|\Delta ct'|}$ in Eq.(A.4) that can be effectively reached in the experiment. The basic experimental features are the uncertainty Δd on the equality of the optical paths, that leads to the condition

$$-\Delta d \leq \Delta ct \leq \Delta d, \tag{A.8}$$

and the acquisition time δt that leads to the condition

$$-\beta \left|\Delta\vec{x}\right| \sin\chi \sin\frac{\pi\delta t}{T} \leq \vec{\beta}\cdot\Delta\vec{x} \leq \beta \left|\Delta\vec{x}\right| \sin\chi \sin\frac{\pi\delta t}{T}, \tag{A.9}$$

where χ is the angle between vector $\vec{V}$ and the polar axis while T is the sidereal day. Eq.(A.9) is obtained (without lack of generality) using the expressions $\Delta\vec{x} = \left|\Delta\vec{x}\right|(1,0,0)$ and $\vec{\beta} = \beta\left(\sin\chi\cos\frac{2\pi t}{T}, \sin\chi\sin\frac{2\pi t}{T}, \cos\chi\right)$ that lead to

$$\vec{\beta}\cdot\Delta\vec{x} = \beta \left|\Delta\vec{x}\right| \sin\chi\cos\frac{2\pi t}{T}. \tag{A.10}$$

From Eq.(A.10) we infer that $\vec{\beta}\cdot\Delta\vec{x}$ is minimized if the acquisition time interval δt is centred on times $t_1 = \frac{T}{4}$ or $t_2 = \frac{3}{4}T$ that is if $t_{1,2} - \frac{\delta t}{2} \leq t \leq t_{1,2} + \frac{\delta t}{2}$. Then, in both cases $\vec{\beta}\cdot\Delta\vec{x}$ in Eq.(A.10) will satisfy conditions (A.9). The minimum value of $\left|\frac{d'_{AB}}{\Delta ct'}\right|$ in Eq.(A.4) ($\beta_{t,min}$ in Eq.(A.7)) occurs if ratio $^{1-\left(\frac{\Delta ct}{d_{AB}}\right)^2}/_{\left(\frac{c\Delta t-\vec{\beta}\cdot\Delta\vec{x}}{d_{AB}}\right)^2}$ is minimized with Δct and $\vec{\beta}\cdot\Delta\vec{x}$ satisfying conditions (A.8) and (A.9). It can be easily seen that this occurs if $(\Delta ct)^2 = (\Delta d)^2$ and $\left(c\Delta t - \vec{\beta}\cdot\Delta\vec{x}\right)^2 = \left(\Delta d + \beta\left|\Delta\vec{x}\right|\sin\chi\sin\frac{\pi\delta t}{T}\right)^2$. Then, we find

$$\beta_{t,min} = \sqrt{1 + \frac{\left(1-\beta^2\right)\left(1-\bar{\rho}^2\right)}{\left(\bar{\rho} + \beta\sin\chi\sin\frac{\pi\delta t}{T}\right)^2}}, \tag{A.11}$$

where $\bar{\rho} \equiv \frac{\Delta d}{d_{AB}}$. Eq.(A.11) just corresponds to Eq.(4).

References

[1] Einstein A, Podolsky B and Rosen N 1935 *Phys. Rev.* **47**(10) 777–780
[2] Bell J S 1964 *Physics* **1** 195–200
[3] Clauser J F, Horne M A, Shimony A and Holt R A 1969 *Phys. Rev. Lett.* **23**(15) 880–884
[4] Clauser J F and Horne M A 1974 *Phys. Rev.* D **10**(2) 526–535
[5] Freedman S J and Clauser J F 1972 *Phys. Rev. Lett.* **28**(14) 938–941
[6] Aspect A, Dalibard J and Roger G 1982 *Phys. Rev. Lett.* **49**(25) 1804–1807
[7] Zeilinger A 1986 *Phys. Lett.* A **118** 1–2
[8] Tittel W, Brendel J, Zbinden H and Gisin N 1998 *Phys. Rev. Lett.* **81**(17) 3563–3566
[9] Weihs G, Jennewein T, Simon C, Weinfurter H and Zeilinger A 1998 *Phys. Rev. Lett.* **81**(23) 5039–5043
[10] Aspect A 1999 *Nature* **398** 189–190
[11] Pan J, Bouwmeester D, Daniell M, Weinfurter H and Zeilinger A 2000 *Nature* **403** 515–519
[12] Grangier P 2001 *Nature* **409** 774–775
[13] Rowe M A, Kielpinski D, Meyer V, Sackett C A, Itano W M, Monroe C and Wineland D J 2001 *Nature* **409** 791–794
[14] Matsukevich D N, Maunz P, Moehring D L, Olmschenk S and Monroe C 2008 *Phys. Rev. Lett.* **100**(15) 150404
[15] Faraci G, Gutkowski D, Notarrigo S and Pennisi A 1974 *Lett. al Nuovo Cim.* **9**(15) 607–611
[16] Clauser J 1976 *Nuovo Cim.* B **33**(2) 740–746
[17] Selleri F 2003 *La fisica nel Novecento: per un bilancio critico* 2nd ed (Bari: Progedit)
[18] Genovese M 2005 *Phys. Rep.* **413** 319–396

[19] Davies P C W and Brown J R 1993 *The ghost in the atom: a discussion of the mysteries of quantum physics* canto ed. ed (Cambridge; New York: Cambridge University Press)

[20] Eberhard P H 1989 A realistic model for quantum theory with a locality property *Quantum theory and pictures of reality: foundations, interpretations, and new aspects* ed Schommers W (Berlin; New York: Springer-Verlag)

[21] Bohm D and Hiley B J 1991 *The undivided universe: an ontological interpretation of quantum mechanics* (Routledge)

[22] Bilaniuk O M P, Deshpande V K and Sudarshan E C G 1962 *Am. J. Phys.* **30** 718–723

[23] Feinberg G 1967 *Phys. Rev.* **159** 1089–1105

[24] Bilaniuk O M P and Sudarshan E C G 1969 *Phys. Today* **22** 43–51

[25] Møller C 1955 *The theory of relativity* (Oxford: Clarendon)

[26] Kowalczyński J 1984 *Int. J. Theor. Phys.* **23**(1) 27–60

[27] Reuse F 1984 *Ann. Phys.* **154** 161–210

[28] Caban P and Rembieliński J 1999 *Phys. Rev.* A **59**(6) 4187–4196

[29] Maudlin T 2001 *Quantum non-locality & relativity* (Oxford: Blackwell)

[30] Cocciaro B 2012 (*Preprint* `1209.3685`)

[31] Anderson R, Vetharaniam I and Stedman G 1998 *Phys. Rep.* **295** 93 – 180

[32] Jammer M 2006 *Concepts of simultaneity from antiquity to Einstein and beyond* (Baltimore, Md.: Johns Hopkins University Press)

[33] Bohm D 1952 *Phys. Rev.* **85**(2) 166–179

[34] Bohm D 1952 *Phys. Rev.* **85**(2) 180–193

[35] Bancal J, Pironio S, Acín A, Liang Y, Scarani V and Gisin N 2012 *Nat. Phys.* **8** 867–870

[36] Gisin N 2012 (*Preprint* `1210.7308`)

[37] Scarani V, Tittel W, Zbinden H and Gisin N 2000 *Phys. Lett.* A **276** 1–7

[38] Salart D, Baas A, Branciard C, Gisin N and Zbinden H 2008 *Nature* **454** 861–864

[39] Cocciaro B, Faetti S and Fronzoni L 2011 *Phys. Lett.* A **375** 379–384

[40] European Gravitational Observatory URL `http://www.ego-gw.it/`

[41] The Virgo collaboration 1997 *Final Design Report* (Virgo Technical Note VIR-TRE-DIR-1000-13)

[42] Altepeter J, Jeffrey E and Kwiat P 2005 *Opt. Express* **13** 8951–8959

[43] Akselrod G M, Altepeter J B, Jeffrey E R and Kwiat P G 2007 *Opt. Express* **15** 5260–5261

[44] Rangarajan R, Goggin M and Kwiat P 2009 *Opt. Express* **17** 18920–18933

[45] Kwiat P G, Waks E, White A G, Appelbaum I and Eberhard P H 1999 *Phys. Rev. A* **60**(2) R773–R776

[46] Resch K *et al.* 2005 *Opt. Express* **13** 202–209

[47] Gisin N, Ribordy G, Tittel W and Zbinden H 2002 *Rev. Mod. Phys.* **74**(1) 145–195

[48] Ciddor Equation URL `http://emtoolbox.nist.gov/wavelength/ciddor.asp`

[49] Peng C Z *et al.* 2005 *Phys. Rev. Lett.* **94** 150501

[50] Aspect A 2002 Bell's theorem: The naive view of an experimentalist *Quantum (Un)speakables: From Bell to Quantum Information* ed Bertlmann R A and Zeilinger A (Springer)